

Cobalt chloride induces apoptosis and zinc chloride suppresses cobalt-induced apoptosis by Bcl-2 expression in human submandibular gland HSG cells

KAZUMI AKITA¹⁻³, HIROHIKO OKAMURA¹, KAYA YOSHIDA¹, HIROYUKI MORIMOTO^{1,4},
HIROAKI OGAWA-IYEHARA² and TATSUJI HANEJI¹

¹Department of Histology and Oral Histology, Institute of Health Biosciences, The University of Tokushima Graduate School, Kuramoto, Tokushima 770-8504; ²Department of Applied Chemistry, Faculty of Engineering, Kyushu Institute of Technology, Kitakyushu 804-8550, Japan

Received April 26, 2007; Accepted June 21, 2007

Abstract. To determine the effects of cobalt chloride on human submandibular gland cells, HSG cells were exposed to various concentrations of cobalt chloride. Cobalt chloride induced cytotoxicity and cell death in HSG cells as determined by phase-contrast microscopy and WST-1 cell viability assay. By using the Hoechst 33342 staining, marked nuclear condensation and fragmentation of chromatin were observed in cobalt chloride-treated cells. Cobalt chloride induced DNA ladder formation in HSG cells in both dose- and time-dependent manner with maximal effect at a concentration of 0.5 mM and 48 h, respectively. Cobalt chloride inhibited the expression of both Bcl-2 protein and mRNA in dose- and time-dependent manner. Zinc chloride recovered the cobalt-suppressed Bcl-2 expression and protected against cobalt-induced apoptosis in HSG cells. Our results show that the pathway of the apoptosis in HSG cells is regulated by cobalt chloride and zinc chloride. Our results also indicate that cobalt-induced apoptotic steps in HSG cells are related to the production of Bcl-2 protein.

Introduction

Apoptosis is one of the essential steps in the maintenance of normal cell populations of adult mammals and occurs

continually in various cell populations. Apoptosis is a morphologically and biochemically distinct mode of cell death that plays major roles during embryogenesis, carcinogenesis, cancer treatment, or immune and toxic cell killing (1-5). The cytologically apparent stages of apoptosis are rapid condensation of chromatin and fragmentation of the cells with membrane-enclosed apoptotic bodies that are phagocytosed and digested by nearby resident cells (6). A biochemical characteristic feature of the process is double-strand cleavage of nuclear DNA at the linker regions between nucleosomes, leading to the production of oligonucleosomal fragments with 180 base pairs, which results in a characteristic laddering pattern on agarose gel electrophoresis (7,8).

Cytotoxicity and genotoxicity of metal compounds have been studied in a variety of systems in human carcinogenesis (9). Among the metal compounds cobalt chloride is registered as a mutagen or genotoxin. Cobalt salt is a minimal or weak mutagen judged by the gene mutation assay with cultured mouse fibroblasts (10,11). However, it showed clear clastogenicity *in vivo* in Syrian hamsters and mice (12). Another cobalt salt, Co (NH₃)₂, did not induce chromosome aberration in the cultured cells (9). These findings suggest that Co (II) ion exerts its genotoxic effect preferentially on *in vivo* systems rather than on *in vitro* systems. Cobalt and other metal chloride were also comparatively assayed in the wing spot test (13).

There is little information on apoptosis in salivary gland cells (14,15), and the role of metal compounds in induction of apoptosis in salivary gland cells remains obscure. To study whether apoptosis in salivary gland cells is related to cobalt ion, human submandibular gland cell line HSG cells, which retain some of the features of salivary gland ductal cells (16,17), was treated with cobalt chloride and apoptosis was studied by morphological and biochemical means.

Materials and methods

Materials. Cobalt chloride, zinc chloride and other metal compounds were purchased from Wako Chemicals (Osaka, Japan). Stock solution (1 M), prepared in Ca²⁺-, Mg²⁺-free

Correspondence to: Dr Tatsuji Haneji, Department of Histology and Oral Histology, Institute of Health Biosciences, The University of Tokushima Graduate School, Kuramoto, Tokushima 770-8504, Japan

E-mail: tat-hane@dent.tokushima-u.ac.jp

Present addresses: ³Kawasumi Laboratories, Inc., Mie-Machi, Ono-gun, Oita 879-7153, Japan; ⁴2nd Department of Anatomy, School of Medicine, University of Occupational and Environmental Health, Kitakyushu 807-8555, Japan

Key words: apoptosis, cobalt, HSG cell, salivary gland, zinc

phosphate-buffered saline (PBS) and protected from light, was diluted to the appropriate concentrations with culture medium. Hoechst 33342 and RNase were purchased from Sigma (St. Louis, MO, USA). Dimethylsulfoxide (DMSO) and Proteinase K were obtained from Merck (Darmstadt, Germany). Dulbecco's modification of Eagle's minimum essential medium (D-MEM) was purchased from Gibco BRL (Gaithersburg, MD, USA). Fetal bovine serum (FBS) was obtained from JRH Biosciences (Lenexa, KS, USA). Plastic dishes were from Iwaki (Chiba, Japan). Anti-Bcl-2 and anti-Bax antibodies were purchased from Santa Cruz Biotechnology (Santa Cruz, CA, USA). Other materials used were of the highest grade commercially available.

Cells and culture conditions. Human submandibular gland ductal cell line HSG cells were provided by Dr Mitsunobu Sato. The cells were grown in plastic dishes containing D-MEM supplemented with 10% (v/v) FBS, 2 mM glutamine, 100 U/ml penicillin, and 100 μ g/ml streptomycin and maintained at 37°C in a humidified atmosphere of 5% CO₂ and 95% air. The cells were subcultured every 7 days using 0.25% trypsin together with 1 mM EDTA in PBS. For experiments, 2x10⁵ cells in 10 ml of medium were plated in 90-mm plastic dishes and incubated for 6 days, at which time the cells were ~90% of confluence. The cells were treated with the agents by adding small volumes of sterile stock solutions to the media and culturing for indicated time. Cell morphology was monitored with an Olympus IMT-2 phase-contrast microscope equipped for photomicroscopy. Phase-contrast microphotographs were taken with Fuji Presto 100 films.

WST-1 assay. The cytotoxicity of HSG cells was analyzed by the WST-1 quantitative colorimetric assay for cell survival (18). The assay detects living, but not dead, cells and the generated signal depends on the degree of activation of the cells. WST-1 reagent (16 mg) and 0.2 mM 1-methoxy-5-methylphenazinium methylsulfate (Cell counting kit, Dojindo Laboratory, Kumamoto, Japan) were dissolved in 100 ml of 20 mM HEPES buffer (pH 7.4). HSG cells grown in 96-well culture plates were treated with the agents for various time periods and washed once with medium. The reaction solution (10 μ l) was immediately added to 100 μ l of a culture medium per well and the cells were then incubated for an additional 90 min at 37°C in a humidified atmosphere of 5% CO₂ and 95% air. The absorbance of each sample was measured at 405 nm with an ImmunoMini NJ-2300 microplate reader (Japan Intermed, Tokyo, Japan). Data were expressed as means \pm SEM. The statistical significance was determined using the Student's t-test calculated by Microsoft Excel 5.0 (Microsoft, Redmond, WA, USA). The level of significance was set at P<0.01.

Nuclear fragmentation assay with Hoechst staining. The cells were plated on sterile 18-mm round glass coverslips placed in 60-mm plastic dishes and cultured. After appropriate cultivation, the coverslips were removed from the dishes and placed directly into 10% formalin in PBS for 10 min at ambient temperature. The fixed cells were washed three times with PBS and permeabilized with methanol for 10 min at -20°C. After washing three times with PBS the coverslips were

incubated with Hoechst 33342 (10 μ g/ml) for 10 min at ambient temperature, rinsed with PBS, and the coverslips were mounted while wet in aqueous mounting medium (Biomedex, Foster City, CA, USA). Cells were examined under an Olympus BX-50 microscope equipped for epifluorescent illumination (BX-FLA). The numbers of apoptotic cells and non-apoptotic cells were counted and the percentages of apoptotic cells were evaluated. Fluorescent photomicrographs were taken on Fuji Presto 400 film using photomicroscopy (PH-30).

DNA isolation and agarose gel electrophoresis. Cells were washed twice in PBS followed by lysis in cold 10 mM Tris-HCl buffer (pH 7.5), 10 mM EDTA, and 0.5% Triton X-100. After cell lysis, debris was removed by centrifugation at 15,000 g for 20 min. RNase was added to the lysates at a final concentration of 20 μ g/ml, and incubated for 1 h at 37°C with gentle shaking. Proteinase K was added to the RNase-treated lysates at a final concentration of 20 μ g/ml. The lysates were further incubated for 1 h at 37°C with gentle shaking. DNA was precipitated with 50% 2-propanol and 0.5 M NaCl overnight at -20°C. After centrifugation and drying, the DNA was dissolved in TE-buffer (10 mM Tris, pH 8.0, containing 1 mM EDTA). Agarose gel electrophoresis of DNA was performed through a 2.0% agarose gel, 100 bp DNA markers (New England BioLabs, Beverly, MA, USA) were run in the same gels. The gels were stained for 10 min with 10 μ g/ml ethidium bromide. To visualize apoptotic alterations to DNA integrity, we observed the DNA bands on an UV transilluminator (Vilber Lourmat, Marnela Vallee, France). Photographs were taken with a Polaroid DS-300 camera.

SDS-PAGE and Western blotting. Cells were washed twice with PBS and scraped into lysate buffer containing 1 mM dithiothreitol, 1 mM phenylmethylsulfonyl fluoride, 1 μ g/ml leupeptin, 2 μ g/ml aprotinin, and 5 mM EGTA in PBS. The cells were sonicated for 10 sec with a sonifier cell disrupter. The sonicates were centrifuged for 10 min at 10,000 g. The supernatants were denatured in sample buffer and heated in boiling water for 5 min. Equal amounts of proteins and prestained molecular weight markers (Gibco BRL) were separated by 12.5% SDS-PAGE and transferred to the polyvinylidene difluoride (PVDF) membranes (Immobilon, Millipore, Bedford, MA, USA). The membranes were incubated for 2 h in a blocking solution containing 5% skim milk in PBS at ambient temperature. The membranes were washed briefly in PBS and incubated overnight in the blocking solution containing a polyclonal anti-Bcl-2 antibody diluted 1:100 or anti-Bax antibody diluted 1:5,000 at 4°C. The membranes were washed four times within 30 min in PBS containing 0.05% Tween-20 using a rotary shaker at ambient temperature. The washed membranes were incubated with horseradish peroxidase (HRP)-conjugated anti-rabbit IgG (diluted 1:3,000 or 1:5,000) in the blocking solution for 2 h at ambient temperature. The membranes were washed as described and the proteins recognised by the antibody were visualised using an ECL detection kit (Amersham Pharmacia Biotech, Uppsala, Sweden) according to the manufacturer's directions.

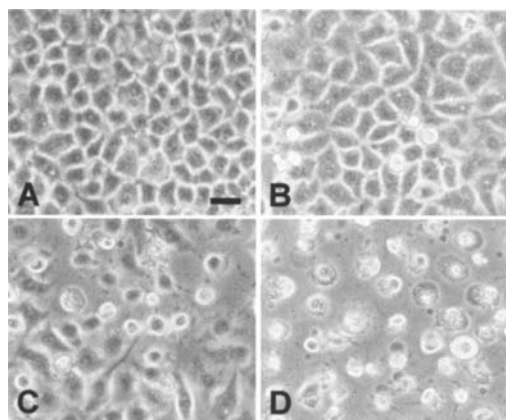


Figure 1. Phase-contrast microphotographs of HSG cells treated with cobalt chloride. After reaching confluence, HSG cells were untreated (A) or treated for 24 h with cobalt chloride at concentrations of 0.1 mM (B), 0.2 mM (C), and 0.5 mM (D). Bar represents 20 μ m.

RNA preparation and reverse transcriptase-polymerase chain reaction (RT-PCR). Total RNA was isolated from HSG cells by Isogen (Nippon Gene, Tokyo, Japan) followed by phenol extraction and ethanol precipitation. Purified RNA was further incubated with DNase I (Sigma) to digest the contaminated DNA. cDNA was synthesised using AMV Reverse Transcriptase XL and Oligo dT-Adaptor Primers (Takara, Osaka, Japan). RT-PCR was performed on the cDNA using the following sense and antisense primers: Bcl-2, sense, 5'-AACAGTCTTCAGGCAAAACG-3'; Bcl-2, antisense, 5'-CTTTTCCTCCACCAAGGTAT-3'. β -actin, sense, 5'-GTGGGGCGCCCCAGGCACCA-3'; β -actin, antisense, 5'-CTCCTTAATGTACGCACGATTTC-3'. Each RT-PCR experiment was carried out using cDNA generated from 0.2 μ g of total RNA. The RT-PCR exponential phase was determined from 30 to 35 cycles to allow semiquantitative comparisons among cDNAs developed from identical reactions. All reactions involved an initial denaturation at 95°C for 10 min followed by at 94°C for 50 sec, 58°C for 50 sec, and 72°C for 50 sec on a Program Temp Control System PC-701 (Astec, Fukuoka, Japan). Reaction was terminated after 5 min elongation step at 72°C. Amplification products were analysed on 2.0% agarose gels and visualised by ethidium bromide staining with a UV transilluminator. Photographs were taken with a Polaroid DS-300 camera.

Results

Effect of cobalt chloride on cell viability in HSG cells. Fig. 1 shows the phase-contrast microphotographs of HSG cells treated with cobalt chloride. Control cultures did not show any cytotoxicity (Fig. 1A). Treatment for 24 h with 0.1 mM cobalt chloride had minimum effect on HSG cell survival as observed under a phase-contrast microscope (Fig. 1B). Cell rounding and shrinking were obvious in the cultures treated with 0.2 mM (Fig. 1C) or 0.5 mM (Fig. 1D) cobalt chloride, indicating that the cells are experiencing cytotoxicity. Morphological changes in HSG cells were not observed by 12 h after 0.5 mM cobalt-treatment (data not shown). At 12 h the cells began to detach from the dishes and at 24 h most cells exhibited

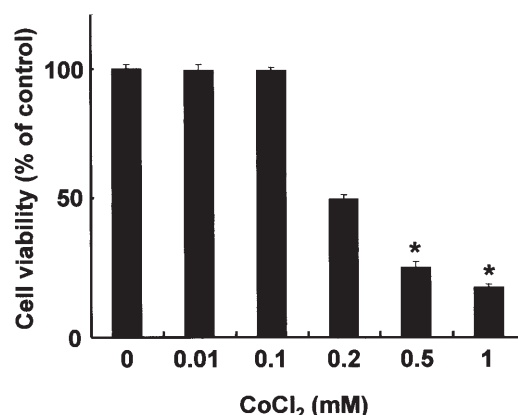


Figure 2. Effects of cobalt chloride on cell viability in HSG cells. HSG cells grown in 96-well plates were treated for 24 h with various concentrations of cobalt chloride and the cell viability was determined by the WST-1 assay. The activity was compared to the control well of the same cell line and results are expressed as a percentage of the control (means \pm SEM) (N=7). The absorbance at 405 nm of the control cultures were 1.089 ± 0.082 . Significant differences from the control cultures are indicated by an asterisk; *P<0.005 (Student's t-test).

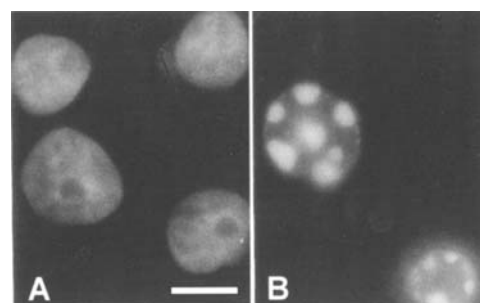


Figure 3. Nuclear morphology of HSG cells. HSG cells were either untreated (A) or treated for 48 h with 0.5 mM cobalt chloride (B). Cells were stained with Hoechst 33342 and observed under a fluorescent microscope. Bar represents 10 μ m.

rounding and shrinking (Fig. 1D). To further quantify the cobalt-induced cell death in HSG cells, cytotoxicity was measured by the WST-1 cell viability assay. Fig. 2 shows that cobalt chloride induced cytotoxicity in HSG cells in a dose-dependent manner up to 1 mM. The level of the cell viability when treated with 0.5 mM cobalt chloride was 25% of the cell viability observed in the control cultures (Fig. 2).

Induction of apoptosis in HSG cells by cobalt chloride. To determine if the cobalt chloride-induced cytotoxicity in HSG cells was due to apoptosis, we evaluated the presence of nuclear fragmentation and condensation in HSG cells treated for 48 h with various concentrations of cobalt chloride. The control cultures of HSG cells (Fig. 3A) did not show any apoptotic features. However, nucleic acid staining with Hoechst 33342 revealed typical apoptotic nuclei, which exhibited highly fluorescent condensed chromatin in the cells treated with 0.5 mM cobalt chloride (Fig. 3B). The number of the cells with nuclear fragmentation increased in response to cobalt chloride in dose- and time-dependent

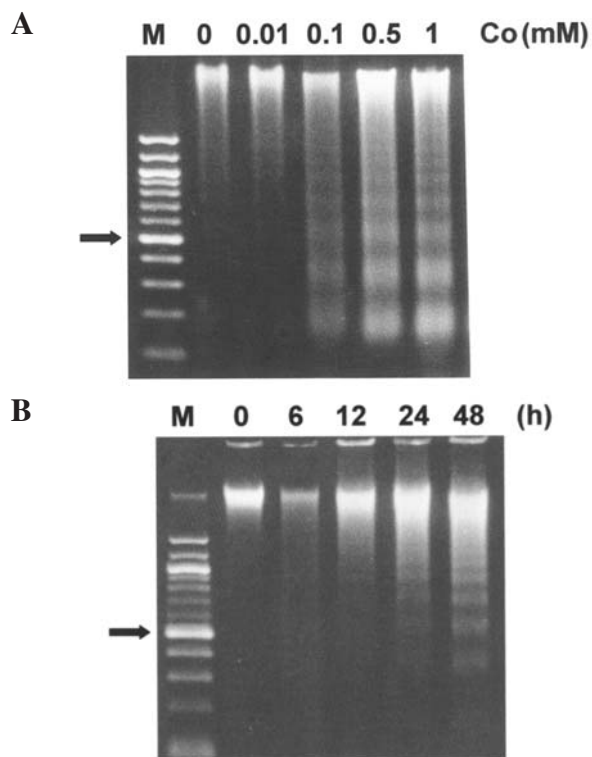


Figure 4. DNA ladder formation in cobalt chloride-treated HSG cells. (A) HSG cells were exposed for 48 h to various concentrations of cobalt chloride as indicated. DNA was extracted and analyzed on an agarose gel. M, standard DNA markers (bp). Arrow indicates 500 bp. (B) HSG cells were exposed to 0.5 mM cobalt chloride for various terms as indicated. DNA was extracted and analyzed on an agarose gel. M, standard DNA markers (bp); Arrow indicates 500 bp.

manner (data not shown). In the HSG cells treated for 48 h with cobalt chloride, a DNA fragmentation pattern forming a ladder of multiples of 180 bp was observed (Fig. 4A). The DNA laddering pattern of the cobalt-treated cells reached a maximal level at 0.5 mM. The time-dependence of the cobalt induced-DNA ladder formation in HSG cells is shown in Fig. 4B. DNA laddering occurred as early as 24 h after cobalt chloride-treatment. The dose- and time-dependence of cobalt-induced DNA ladder formation was comparable to that of the cytotoxicity obtained from WST-1 assay.

Effects of zinc chloride on cobalt chloride-induced apoptosis in HSG cells. HSG cells were treated for 24 h with various concentrations of zinc chloride with or without 0.5 mM cobalt chloride. Zinc chloride increased the cobalt-suppressed cell viability in HSG cells in a dose-dependent manner up to 100 μ M measured by WST-1 assay (Fig. 5A). Cell viability of the cultures co-treated with zinc chloride and cobalt chloride was three times higher than that of the cobalt-treated cells. Zinc chloride alone at the doses used did not show any cytotoxicity in HSG cells. Fig. 5B shows an agarose gel of electrophoresed DNA isolated from the HSG cells treated for 48 h with various concentrations of zinc chloride under a fixed dose of cobalt chloride (0.5 mM). In the cobalt-treated cells, DNA ladder formation was obvious; however, the degree of DNA laddering decreased as the concentrations of zinc chloride increased. Zinc chloride at 100 μ M completely recovered the cobalt-induced DNA laddering and no ladder

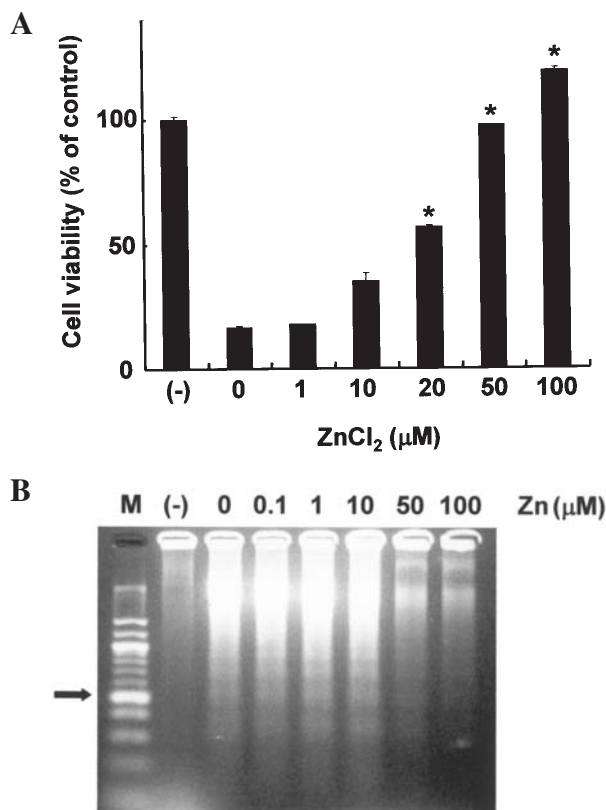


Figure 5. Effects of zinc chloride on cobalt chloride-treated HSG cells. (A) HSG cells grown in 96-well plates were treated for 24 h with 0.5 mM cobalt chloride and various concentrations of zinc chloride. The mitochondrial activities of the living cells were determined by WST-1 assay. The cell viability was compared with those in the control cultures and expressed as percentage of the control (means \pm SEM) (N=7). The absorbance at 405 nm of the control cultures were 1.107 ± 0.096 . (-), Cultures without cobalt chloride and zinc chloride. * $P < 0.005$, compared with the cultures treated with cobalt chloride only. (B) Zinc chloride protects cobalt-induced DNA ladder formation in HSG cells. HSG cells were exposed for 48 h to various concentrations of zinc chloride under a fixed dose of 0.5 mM cobalt chloride. DNA was extracted and run in the agarose gel. M, Standard DNA markers (bp); (-), Cultures without cobalt chloride and zinc chloride. Arrow indicates 500 bp.

formation was detected. The same concentrations of zinc chloride had no effects on DNA ladder formation (data not shown).

Prevention of Bcl-2 expression by cobalt chloride and recovery of the cobalt-suppressed Bcl-2 expression by zinc chloride. Fig. 6 shows the reaction between the anti-Bcl-2 and anti-Bax antibodies and the proteins extracted from the 0.5 M cobalt-treated HSG cells. Anti-Bcl-2 antibody interacted with a band having an estimated molecular weight of 43 kDa. HSG cells expressed detectable level of Bcl-2 protein at the confluent stage. The staining intensity of Bcl-2 protein time-dependently decreased in the cell lysates prepared from the 0.5 mM cobalt-treated cells (Fig. 6). The staining intensity of Bax protein did not change in the lysates from the cells treated with 0.5 mM cobalt chloride up to 48 h. The corresponding band was not detected in the extracts of the cells incubated with the same dilution of normal rabbit serum (data not shown).

Fig. 7 shows that zinc chloride restored the cobalt-suppressed expression of Bcl-2 protein. HSG cells expressed

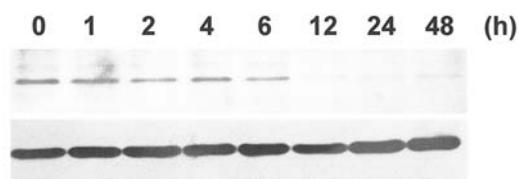


Figure 6. Western blot analysis of Bcl-2 and Bax protein in cobalt chloride-treated HSG cells. HSG cells were treated with 0.5 mM cobalt chloride for the variable time periods as indicated and cell lysates were prepared. Ten microgram samples were separated on a 12.5% of SDS-PAGE gel and transferred to PVDF membranes. Each membrane was then incubated with anti-Bcl-2 (upper panel) or anti-Bax (lower panel) antibodies.

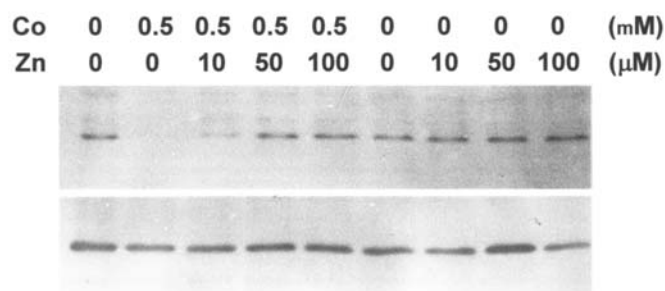


Figure 7. Effects of zinc chloride on cobalt-suppressed expression of Bcl-2 protein. HSG cells were treated for 24 h with or without 0.5 mM cobalt chloride and various concentrations of zinc chloride as indicated. The samples were analyzed by Western blotting using anti-Bcl-2 (upper panel) or anti-Bax (lower panel) antibodies.

detectable level of Bcl-2 protein at the confluent stage. In the cells treated for 24 h with 0.5 mM cobalt chloride, the level of Bcl-2 protein was low, however, zinc chloride increased the level of Bcl-2 protein in a dose-dependent manner. Treatment of zinc chloride at 100 μ M completely recovered the cobalt-suppressed Bcl-2 protein expression to the control level. Fig. 7 also shows that the same amounts of zinc chloride did not alter the expression of Bcl-2 protein.

Expression of Bcl-2 mRNA in HSG cells treated with cobalt chloride and zinc chloride. Bcl-2 mRNA was constitutively expressed in HSG cells, as judged from the results obtained by RT-PCR method. Approximately 480 bp band for the specific primers for Bcl-2 mRNA used in the present study was detected in HSG cells after amplification of cDNA for 35 cycles. The RT-PCR exponential phase was determined from 31 to 34 cycles to allow semiquantitative comparisons among cDNAs developed from identical reactions. Semiquantitative analysis of Bcl-2 mRNA was done with the mRNA amplified by 33 cycles in HSG cells treated with 0.5 mM cobalt chloride for various time-points. Fig. 8 shows that the expression of Bcl-2 mRNA decreased in a time-dependent manner up to 8 h. The RT-PCR product of β -actin prepared from the same samples and amplified for the same number of cycles is also shown in Fig. 8. There were no quantitative differences in the PCR product of β -actin between the cells treated with different concentrations of cobalt chloride. Fig. 9 shows that zinc chloride enhanced the mRNA expression of Bcl-2 in HSG cells that was suppressed by the cobalt treatment. The

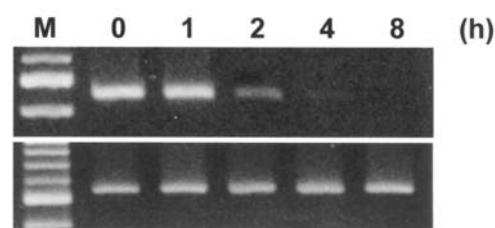


Figure 8. Expression of Bcl-2 mRNA in HSG cells treated with cobalt chloride. HSG cells were treated for various time periods with cobalt chloride as indicated and semiquantitative analysis of Bcl-2 mRNA was done with the mRNA amplified by 33 cycles in HSG cells (upper panel). The RT-PCR product of β -actin prepared from the same samples and amplified for the same number of cycles is also shown in lower panel. M, Standard DNA markers (bp).

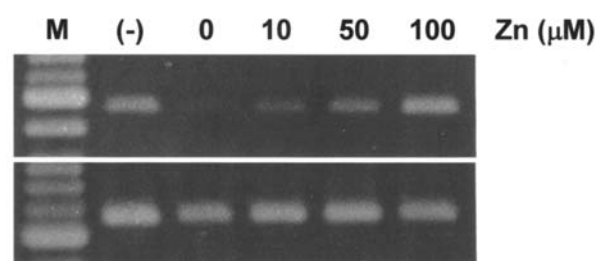


Figure 9. Effects of zinc chloride on cobalt-suppressed expression of Bcl-2 mRNA. HSG cells were treated for 8 h with various concentrations of zinc chloride under a fixed dose of cobalt chloride (0.5 mM). M, Standard DNA markers (bp); (-), Cultures without cobalt chloride and zinc chloride. Total RNA was prepared and RT-PCR was conducted. Semiquantitative analysis of Bcl-2 mRNA was done with the mRNA amplified by 33 cycles in HSG cells (upper panel). The RT-PCR product of β -actin prepared from the same samples and amplified for the same number of cycles is also shown in lower panel.

maximum stimulation was observed at 100 μ M zinc chloride. The same concentrations of zinc chloride without cobalt chloride did not alter the Bcl-2 mRNA expression (data not shown). The β -actin mRNA was constitutively expressed, and its level was not affected by the treatment of zinc chloride.

Discussion

In the present study, we treated HSG cells with various concentrations of cobalt chloride for various time-points to examine whether this metal compound could induce apoptosis in these cells. Obvious morphological changes were observed in HSG cells treated with cobalt chloride by phase-contrast microscopy. Loss of cell viability in cobalt-treated cells was also demonstrated by the WST-1 cell viability assay. By using the Hoechst 33342 staining, marked nuclear condensation and fragmentation into spherical bodies were demonstrated. Moreover, DNA ladder formation was detected in HSG cells treated with cobalt chloride. These results indicate that cobalt chloride induced apoptosis in HSG cells. Effect of cobalt chloride on induction of apoptosis is not limited to HSG cells because cobalt chloride also induced apoptosis in human osteosarcoma cell lines, Saos-2 cells and MG63 cells, human squamous carcinoma SCC-25 cells, and CHO cells (Hiromatsu *et al*, unpublished data). These findings are in

good agreement with the past reports concerning their biological effects in other systems (19-21). It was reported that cobalt chloride induced DNA ladder formation in HL-60 cells but not in human gingival fibroblasts (22). These findings together with our present results suggest that the pathway of cobalt-induced apoptosis might be different in the cells examined. The mechanisms of the cobalt-induced apoptotic pathway should be examined in details.

Some metal ions were reported to have cytotoxic activity and induce apoptosis in certain cell types (23). Cobalt chloride was reported to induce hypoxia environment, stimulate the expression of hypoxia-inducible factor-1 α (HIF-1 α), and induce apoptosis in cultured cells probably via a PI3 kinase/Akt pathway (24-26). However, it was reported that hypoxia induced (27) or protected apoptosis (28) in cultured cells via HIF-1 α -independent pathways.

HIF-1 α was also reported to stabilise wild-type p53 onco-suppressor protein (29). Since p53 is expressed in HSG cells (30), cobalt-induced apoptosis in HSG cells may play a role related to p53. It has also been reported that apoptosis is related to p53, which induces redox-related genes and formation of reactive oxygen species (31). In our preliminary results, the antioxidants including ascorbic acid and cysteine protected against the cobalt-induced apoptosis in HSG cells. Cobalt-induced apoptosis in HSG cells demonstrated in the present study might play a role in at least one pathway related to reactive oxygen species.

Members of the Bcl-2 protein family play important roles in regulating apoptosis. Bcl-2 protein is probably the best studied apoptotic suppressor and it is known to prevent apoptosis in response to a large variety of stimuli. The effects of Bcl-2 protein on apoptosis were determined by its interaction with Bax. Bax promotes apoptosis by inducing loss of the electrochemical gradient across the inner membrane of mitochondria and participates in the formation of the mitochondrial pores, which influence the release of cytochrome c, AIF, or smac/Diablo. All these effects are suppressed by Bcl-2. In the present study, we demonstrated that cobalt chloride decreased the expression of Bcl-2 both at transcriptional and translational levels. Cobalt chloride was reported to decrease the level of Bcl-2 protein in human U937 macrophages (32). Bcl-2 protein may share the same signaling pathway with Fas receptor and interferes with the apoptotic process mediated by the Fas receptor (33). If cobalt chloride induces down-regulation of Bcl-2 protein, Fas receptor and Fas ligand expression stimulated by cobalt chloride might promptly induce apoptosis (34). Cobalt chloride also induced apoptosis via protein kinase and caspase activation (35,36).

We demonstrated that zinc chloride protected the cobalt-induced apoptosis in HSG cells. Zinc chloride restored the cobalt-suppressed expression of Bcl-2 in HSG cells. It was reported that zinc chloride inhibited apoptosis by suppressing Bcl-2 expression in cultured human prostate epithelial cells (37). Zinc may act in the early phases of the apoptotic pathway, before the activation of caspase cascades leading to DNA fragmentation and degradation (38-40). These results are in line with the inhibition of H₂O₂-induced apoptosis by zinc, parallel to decrease of Bax expression in U937 cells (41). It was reported that zinc inhibited Bax and Bak activation and cytochrome c release induced by chemical inducers of

apoptosis (42). The regulation of mitochondrial proteins is not the only target of zinc (43). Zinc is able to act at different levels on the apoptotic pathway. It was shown that zinc prevented ricin-induced apoptosis by an inhibition of the increase of caspases 3, 6, and 9 in U937 cell line (44). The induction of metallothionein was also postulated as a mechanism involved in the anti-apoptotic effects of zinc, but the induction of metallothioneins by zinc requires pre-treatment of cells with this metal (45). Anti-apoptotic properties of zinc have often been compared to Bcl-2 anti-apoptotic properties. They can both prevent caspase cascades and protect cells from oxidative stress (46,47). Our results together with those of others suggest that an increase of the Bcl-2 protein can be a target for zinc in relation to its anti-apoptotic properties. In further experiments, it would be worth studying the mechanisms of the regulation of Bcl-2 by zinc chloride. Zinc has been shown to enhance the transcriptional activity of some genes, which contain specific zinc-finger regions. To our knowledge, however, no studies have shown that Bcl-2 gene could have a metal-response element in its promoter/enhancer regions. Proteins that play a role in apoptosis are numerous and a better understanding of their mechanisms is necessary to know how these proteins interact with zinc, because intracellular zinc levels influence cell survival (23,43). Studies of the anti-apoptotic properties of zinc are important lines of research, not only in disease where zinc homeostasis is often distorted, but also in the comprehension of cancer mechanisms, where inhibition of apoptotic process may be involved.

During salivary gland development, acinar cells are thought to arise from pluripotent stem cells derived from the intercalated ductal cells (48). HSG cells have characteristics of intercalated duct cells (16,17) and differentiate to acinar cells, fluid-secreting cells of salivary gland (14). HSG cells also are able to mimic several features of the Sjögren's syndrome process and apoptosis in these cells is induced by treatment with interferon- γ (15). Primary Sjögren's syndrome is a chronic autoimmune disease of salivary glands, which produce little or no saliva because of the absence of acinar cells. Our findings suggest that metal ions including cobalt and zinc may be significant factors in the function and regulation of salivary glands, including normal growth and repair processes, pathogenesis of Sjögren's syndrome, or apoptosis.

References

1. Arends MJ and Wyllie AH: Apoptosis: mechanisms and roles in pathology. *Int Rev Exp Pathol* 32: 223-254, 1991.
2. Kerr JFR, Winterford CM and Harmon BV: Apoptosis: its significance in cancer and cancer therapy. *Cancer* 73: 2013-2026, 1994.
3. Jacobson MD, Weil M and Raff MC: Programmed cell death in animal development. *Cell* 88: 347-354, 1997.
4. Haneji T: Association of protein phosphatase 1 delta with nucleolin in osteoblastic cells and cleavage of nucleolin in apoptosis-inducing osteoblastic cells. *Acta Histochem Cytochem* 38: 1-8, 2005.
5. Okamura H, Yoshida K, Morimoto H and Haneji T: PTEN expression elicited by *EGR-1* transcription factor in calyculin A-induced apoptotic cells. *J Cell Biochem* 94: 117-125, 2005.
6. Savill J and Fadok V: Corpse clearance defines the meaning of cell death. *Nature* 407: 784-788, 2000.
7. Wyllie AH: Glucocorticoid-induced thymocyte apoptosis is associated with endogenous endonuclease activation. *Nature* 284: 555-556, 1980.

8. Gong J, Traganos F and Darzynkiewicz Z: A selected procedure for DNA extraction from apoptotic cells applicable for gel electrophoresis and flow cytometry. *Anal Biochem* 218: 314-319, 1994.
9. Paton GR and Allison AC: Chromosome damage in human cell cultures induced by metal salts. *Mutat Res* 16: 332-336, 1972.
10. Morita H, Umeda M and Ogawa HI: Mutagenicity of various chemicals including nickel and cobalt compounds in cultured mouse FM3A cells. *Mutat Res* 261: 131-137, 1991.
11. Kasten U, Hartwig A and Beyersmann D: Mechanisms of cobalt (II) uptake into V79 Chinese hamster cells. *Arch Toxicol* 66: 592-597, 1992.
12. Palit S, Sharma A and Talukder G: Chromosomal aberrations induced by cobaltous chloride in mice *in vivo*. *Biol Trace Elem Res* 29: 139-145, 1991.
13. Ogawa-Iyehara H, Shibahara T, Iwata H, *et al*: Genotoxic activities *in vivo* of cobaltous chloride and other metal chlorides as assayed in the *Drosophila* wing spot test. *Mutat Res* 320: 133-140, 1994.
14. Hoffman MP, Kibbey MC, Letterio JJ and Kleinman HK: Role of laminin-1 and TGF- β 3 in acinar differentiation of a human submandibular gland cell line (HSG). *J Cell Sci* 109: 2013-2021, 1996.
15. Wu AJ, Chen ZJ, Tsokos M, O'Connell BC, Ambudkar IS and Baum BJ: Interferon- γ induced cell death in a cultured human salivary gland cell line. *J Cell Physiol* 167: 297-304, 1996.
16. Shirasuna K, Sato M and Miyazaki T: A neoplastic epithelial duct cell line established from an irradiated human salivary gland. *Cancer* 48: 745-752, 1981.
17. Sato M, Hayashi Y, Yoshida H, Yanagawa T, Yura Y and Nitta T: Search for specific markers of neoplastic epithelial duct and myoepithelial cell lines established from human salivary gland and characterization of their growth *in vitro*. *Cancer* 54: 2959-2967, 1984.
18. Takenouchi T and Munekata E: Trophic effects of substance P and β -amyloid peptide on dibutyryl cyclic AMP-differentiated human leukemic (HL-60) cells. *Life Sci* 56: 479-484, 1995.
19. Costa M: Levels of ornithine decarboxylase activation used as a simple marker of metal induced growth arrest in tissue culture. *Life Sci* 24: 705-713, 1979.
20. Lin PS, Kwock L, Hefter K and Misslbeck G: Effects of iron, copper, cobalt, and their chelators on the cytotoxicity of bleomycin. *Cancer Res* 43: 1049-1053, 1983.
21. Wataha JC, Hanks CT and Craig RG: The *in vitro* effects of metal cations on eukaryotic cell metabolism. *J Biomed Mater Res* 25: 1133-1149, 1991.
22. Schedle A, Samorapoompichit P, Rausch-Fan XH, Franz A, Fureder W, Sperr WR, Sperr W, Ellinger A, Slavicek R, Boltz-Nitulescu G and Valent P: Response of L-929 fibroblasts, human gingival fibroblasts, and human tissue mast cells to various metal cations. *J Dent Res* 74: 1513-1520, 1995.
23. Pulido MD and Parrish AR: Metal-induced apoptosis: mechanisms. *Mutat Res* 533: 227-241, 2003.
24. Vengellur A and La Pres JJ: The role of hypoxia inducible factor 1 α in cobalt chloride induced cell death in mouse embryonic fibroblasts. *Toxicol Sci* 82: 638-646, 2004.
25. Gross J, Fuchs J, Machulik A, Jahnke V, Kietzmann T and Bockmuhl U: Apoptosis, necrosis and hypoxia inducible factor-1 in human head and neck squamous cell carcinoma cultures. *Int J Oncol* 27: 807-814, 2005.
26. Ardyanto TD, Osaki M, Tokuyasu N, Nagahama Y and Ito H: CoCl₂-induced HIF-1 α expression correlates with proliferation and apoptosis in MKN-1 cells: a possible role for the PI3K/Akt pathway. *Int J Oncol* 29: 549-555, 2006.
27. Guo M, Song LP, Jiang Y, Liu W, Yu Y and Chen GQ: Hypoxia-mimetic agents desferrioxamine and cobalt chloride induce leukemic cell apoptosis through different hypoxia-inducible factor-1 α independent mechanisms. *Apoptosis* 11: 67-77, 2006.
28. Piret JP, Cosse JP, Ninane N, Raes M and Michiels C: Hypoxia protects HepG2 cells against etoposide-induced apoptosis via a HIF-1-independent pathway. *Exp Cell Res* 312: 2908-2920, 2006.
29. An WG, Kanekal M, Simon MC, Maltepe E, Blagosklonny MV and Neckers LM: Stabilization of wild-type p53 by hypoxia-inducible factor 1 α . *Nature* 392: 405-408, 1998.
30. McArthur CP, Wang Y, Heruth D and Gustafson S: Amplification of extracellular matrix and oncogenes in tat-transfected human salivary gland cell lines with expression of laminin, fibronectin, collagens I, III, IV, c-myc and p53. *Arch Oral Biol* 46: 545-555, 2001.
31. Polyak K, Xia Y, Zweier JL, Kinzler KW and Vogelstein B: A model for p53-induced apoptosis. *Nature* 389: 237-238, 1997.
32. Petit A, Mwale F, Zukor DJ, Catelas I, Antoniou J and Huk OL: Effect of cobalt and chromium ions on bcl-2, bax, caspase-3, and caspase-8 expression in human U937 macrophages. *Biomaterials* 25: 2013-2018, 2004.
33. Itoh N, Tsujimoto Y and Nagata S: Effect of bcl-2 on Fas antigen-mediated cell death. *J Immunol* 151: 621-627, 1993.
34. Jung JY and Kim WJ: Involvement of mitochondrial- and Fas-mediated dual mechanism in CoCl₂-induced apoptosis of rat PC12 cells. *Neurosci Lett* 371: 85-90, 2004.
35. Zou W, Zeng J, Zhuo M, Sun L, Wang J and Liu X: Involvement of caspase-3 and p38 mitogen-activated protein kinase in cobalt chloride-induced apoptosis in PC12 cells. *J Neurosci Res* 67: 837-843, 2002.
36. Kim HJ, Yang SJ, Kim YS and Kim TU: Cobalt chloride-induced apoptosis and extracellular signal-regulated protein kinase activation in human cervical cancer HeLa cells. *J Biochem Mol Biol* 36: 468-474, 2003.
37. Untergasser G, Rumpold H, Plas E, Witkowski M, Pfister G and Berger P: High levels of zinc ions induce loss of mitochondrial potential and degradation of antiapoptotic Bcl-2 protein in *in vitro* cultivated human prostate epithelial cells. *Biochem Biophys Res Commun* 279: 607-614, 2000.
38. Schrantz N, Auffredou MT, Bourgeade MF, Besnault L, Leca G and Vazquez A: Zinc-mediated regulation of caspase activity: dose-dependent inhibition or activation of caspase-3 in the human Burkitt lymphoma B cells (Ramos). *Cell Death Differ* 8: 152-161, 2001.
39. Maire MA, Rast C, Pagnout C and Vasseur P: Changes in expression of bcl-2 and bax in Syrian hamster embryo (SHE) cells exposed to ZnCl₂. *Arch Toxicol* 79: 90-101, 2005.
40. Mann JJ and Fraker PJ: Zinc pyrithione induces apoptosis and increases expression of Bim. *Apoptosis* 10: 369-379, 2005.
41. Fukamachi Y, Karasaki Y, Sugiura T, Itoh H, Abe T, Yamamura K and Higashi K: Zinc suppresses apoptosis of U937 cells induced by hydrogen peroxide through an increase of the Bcl-2/Bax ratio. *Biochem Biophys Res Commun* 246: 364-369, 1998.
42. Ganju N and Eastman A: Zinc inhibits Bax and Bak activation and cytochrome c release induced by chemical inducers of apoptosis but not by death-receptor-initiated pathways. *Cell Death Differ* 10: 652-661, 2003.
43. Feng P, Li TL, Guan ZX, Franklin RB and Costello LC: Direct effect of zinc on mitochondrial apoptogenesis in prostate cells. *Prostate* 52: 311-318, 2002.
44. Tamura T, Sadakata N, Oda T and Muramatsu T: Role of zinc ions in ricin-induced apoptosis in U937 cells. *Toxicol Lett* 132: 141-151, 2002.
45. Shimoda R, Achanzar WE, Qu W, Nagamine T, Takagi H, Mori M and Waalkes MP: Metallothionein is a potential negative regulator of apoptosis. *Toxicol Sci* 73: 294-300, 2003.
46. Truong-Tran AQ, Carter J, Ruffin RE and Zalewski PD: The role of zinc in caspase activation and apoptotic cell death. *Biomaterials* 14: 315-330, 2001.
47. Ostrakhovitch EA and Cherian MG: Role of p53 and reactive oxygen species in apoptotic response to copper and zinc in epithelial breast cancer cells. *Apoptosis* 10: 111-121, 2005.
48. Yagil C, Michaeli Y and Zahuzej G: Compensatory proliferative response of the rat submandibular salivary gland to unilateral extirpation. *Virchows Arch B Cell Pathol* 49: 83-91, 1985.